

## Identification of impurities in ivermectin bulk material by mass spectrometry and NMR

Christopher A. Beasley<sup>a</sup>, Tsang-Lin Hwang<sup>b</sup>, Kyle Fliszar<sup>a</sup>, Andreas Abend<sup>a,\*</sup>,  
David G. McCollum<sup>c</sup>, Robert A. Reed<sup>a</sup>

<sup>a</sup> Pharmaceutical Research and Development, Merck Research Laboratories, Merck & Co., Inc., WP78-210, West Point, PA 19486, USA

<sup>b</sup> Bioprocess and Bioanalytical Research, Merck Research Laboratories, Merck & Co., Inc., WP78-107, West Point, PA 19486, USA

<sup>c</sup> Analytical Sciences and Technology, Pfizer Global Manufacturing, Mail Stop 4851-259-175, 7000 Portage Road, Kalamazoo, MI 49001, USA

Received 26 October 2005; received in revised form 7 February 2006; accepted 8 February 2006

Available online 22 March 2006

### Abstract

The identification and characterization of four process impurities in bulk ivermectin and four process impurities in bulk avermectin, using a combination of MS and NMR, are discussed herein. These process impurities were shown to be 24-demethyl H<sub>2</sub>B<sub>1a</sub>, 3'-demethyl H<sub>2</sub>B<sub>1a</sub>, 3''-demethyl H<sub>2</sub>B<sub>1a</sub> and 24a-hydroxy B<sub>2a</sub> isomer. The impurities were shown to be process impurities and are present in avermectin bulk also.

© 2006 Elsevier B.V. All rights reserved.

**Keywords:** HPLC; Ivermectin; Avermectin; Process impurities; NMR; MS

### 1. Introduction

The actinomycete *Streptomyces avermitilis* produces a potent class of anthelmintic compounds known as avermectins [1]. These compounds have a broad pharmacological spectrum against a wide variety of endo and ecto parasites including nematodes and arthropods. The avermectins are comprised of several structurally very similar compounds (Fig. 1) which consist of a 16-membered macrocyclic lactone ring, which is attached to a spiroketal unit spanning from C17–C27 and to a hexahydrobenzofuran unit (C2–C8a). In contrast to the structurally related milbemycins and nemadectin (the chemical precursor of the active ingredient moxidectin), which also have a 16-membered lactone ring motif, the avermectins contain a characteristic disaccaride side-chain. Loss of the disaccaride side-chain in avermectin reduces their pharmacological activity. The avermectins can be subdivided into a two compound classes, one contains a methoxy moiety at C5 (avermectin “A”), and one contains a hydroxyl group at C5 (avermectin “B”). The avermectins “A” and “B” can be further subdivided into four compound classes

known as “A1”, “A2”, “B1”, and “B2”. The “A1” and “B1” class of compounds bears an unsaturated bond between C22 and C23. Addition of water to the C22–23 double bond in avermectins “A1” and “B1” formally produces the avermectins “A2” and “B2”, with the hydroxyl group attached to C23. Each of the four subgroups (“A1”, “A2”, “B1”, “B2”) can be further divided into two compound classes, which are characterized by an ethyl substituent (denoted “A<sub>1a</sub>”, “B<sub>1a</sub>”, “A<sub>2a</sub>”, “B<sub>2a</sub>”) or methyl substituent at C27 (“A<sub>1b</sub>”, “B<sub>1b</sub>”, “A<sub>2b</sub>”, “B<sub>2b</sub>”). Commercial grade avermectin consists of avermectins A<sub>1a</sub> and A<sub>1b</sub>, which are isolated from *Streptomyces avermitilis* fermentations through several extractions, precipitations and chromatographic separations [2–4].

Avermectin has been used as starting material and molecular template for the production of several newly designed anti-parasitic drugs with different pharmacological applications or with enhanced safety profiles. Ivermectin is produced via catalytic hydrogenation of avermectin B<sub>1a</sub> and B<sub>1b</sub> at the C22–C23 double bond and abbreviated H<sub>2</sub>B<sub>1a</sub> and H<sub>2</sub>B<sub>1b</sub>. This compound is by far the most successful avermectin derived active pharmaceutical ingredient and used in a number of veterinary health care products [5–11]. Furthermore, ivermectin containing formulations are also used for the treatment of onchocerciasis [12,13] (river blindness), threadworm infestation [14] usually as

\* Corresponding author. Tel.: +1 215 652 6910; fax: +1 215 652 2835.

E-mail address: [andreas\\_abend@merck.com](mailto:andreas_abend@merck.com) (A. Abend).

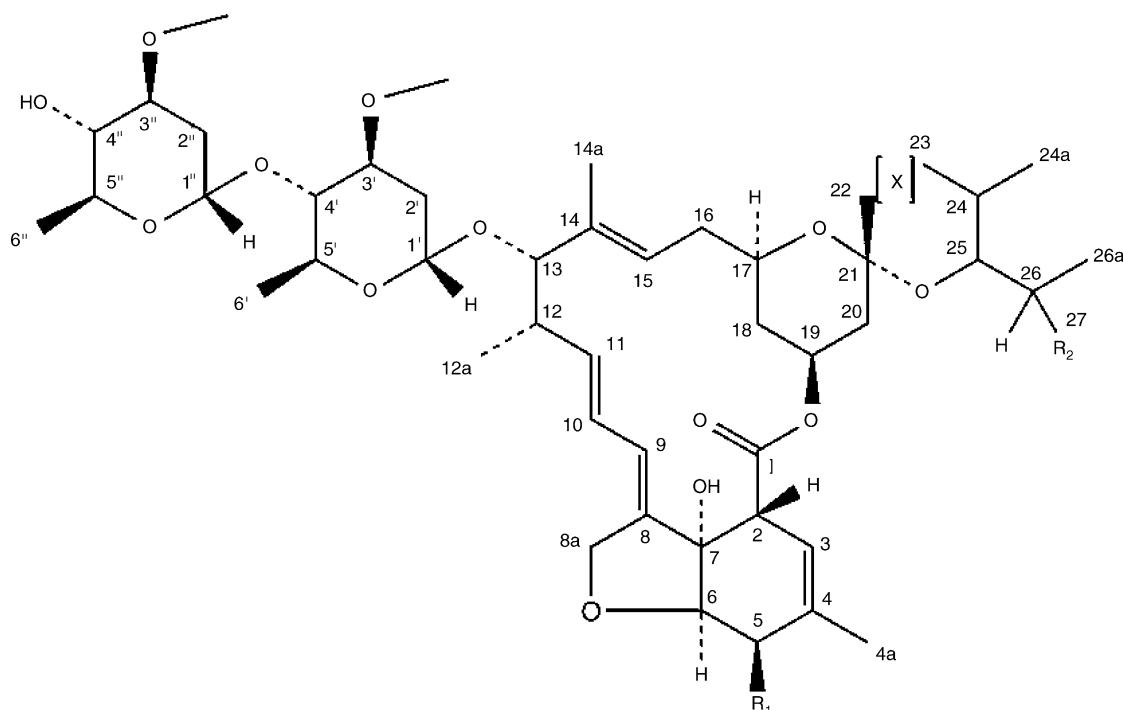


Fig. 1. A components:  $R_1 = \text{OCH}_3$ ; B components:  $R_1 = \text{OH}$ ; a components:  $R_2 = \text{C}_2\text{H}_5$ ; b components:  $R_2 = \text{CH}_3$ ; 2 components:  $X = \text{CH}_2\text{CHOH}$ ; 1 components:  $X = \text{CHCH}$ .

a result of raw fish consumption in humans, and dermatological conditions [15,16]. Other semi-synthetic derivatives of avermectin include eprinomectin [17–22] and emamectin benzoate [23–26] which were introduced recently as active ingredients in veterinary formulations or for crop protection. These compounds are prepared by substitution of the 4'' hydroxy group in avermectin B<sub>1a</sub> and B<sub>1b</sub> with an amino (eprinomectin) or an amino-methyl group (emamectin benzoate). Another attractive way to produce novel avermectins with new or enhanced properties is through genetic engineering. Doramectin, in which the branched aliphatic side-chain (C23–C27) characteristic of avermectins is replaced by a cyclohexane ring, is produced via a fermentation process in genetically engineered *S. avermitilis* and represents another important commercial avermectin derivative [27].

As described in the European Pharmacopeia [28] and USP [29] monographs on ivermectin, pharmaceutical grade ivermectin is a mixture of no less than 90% H<sub>2</sub>B<sub>1a</sub> and no more than 10% H<sub>2</sub>B<sub>1b</sub> with total content (H<sub>2</sub>B<sub>1a</sub> + H<sub>2</sub>B<sub>1b</sub>) of 95.0–102.0%. Included in the EP monograph are acceptance criteria on impurities, whether they be degradation products or process impurities, several of which remain unidentified. Mass spectrometry and NMR characterizations of avermectins, including ivermectin, some impurities, and related degradation products have been reported [30–34]. We describe herein the purification by HPLC followed by identification using APCI–MS/MS and NMR for several yet to be identified process impurities in ivermectin. These newly identified impurities can be traced back to avermectin and may be relevant to other semi-synthetic and genetically engineered avermectins as well.

## 2. Experimental

### 2.1. Chemicals and reagents

Ivermectin and avermectin bulk drug was obtained from Merck & Co., Inc. (Whitehouse Station, NJ). Acetonitrile and methanol were HPLC grade and obtained from Fisher Scientific (Norristown, PA). CDCl<sub>3</sub> (99.8%) and CD<sub>3</sub>OD (99.8%) were obtained from Isotec Inc. (Miamisburg, OH).

### 2.2. Equipment

#### 2.2.1. Instruments

Separations were carried out on an Agilent (Palo Alto, CA) 1100 series HPLC system equipped with a QuatPump G1311A, diode array detector (DAD) G1315A, column heater G1316A and degasser G1322A. The HPLC system was remotely controlled via a PC. Data and on-line UV spectral acquisition as well as data analysis was performed using Agilent's ChemStation software (Version A.01.01 [682]). Analytical columns used to achieve separation were the Phenomenex (Torrance, CA) Luna C18 (2) (150 mm × 4.6 mm ID, 3 μm) and Jones Chromatography (Foster City, CA) Apex ODS (250 mm × 4.6 mm ID, 5 μm). Column temperature was 40 °C, and detection wavelengths were 245 and 280 nm. Mobile phase composition and injection volumes are as stated throughout the text.

An Agilent 1100 series HPLC system consisting of Prep-Pump G1361A (2×), DAD 1315B, ALS Therm G1330B, AFC G1364A and manual injection valve Rheodyne 37251-038 was used for preparative-scale separations. The HPLC system was remotely controlled via a PC. Data and on-line

UV spectral acquisition as well as data analysis was performed using Agilent's ChemStation software (Version A.10.01 [1635]). The preparative column used was a Phenomenex Luna C18 (250 mm  $\times$  10 mm ID, 5  $\mu$ m). The injection volume for preparative-scale separation was 3 mL. Column temperature was not controlled and detection wavelengths were 245 and 280 nm. Individual fractions from preparative separations were concentrated and dried using a Vacuubrand (Cedar Grove, NJ) Vario PC2001 rotary evaporator equipped with a Fisher Scientific Isotemp 910 refrigerated circulator set at 4 °C. Samples were further dried using a Schlenk line apparatus equipped with a 1/2 HP Franklin Electric (Bluffton, IN) vacuum pump.

Liquid chromatography/mass spectrometry (LC/MS<sup>n</sup>) experiments were carried out on an Agilent 1100 series HPLC equipped with BinPump G1312A, DAD G1315B, column heater G1316A and degasser G1322A. An LCQ from Thermo-Electron (Waltham, MA) was equipped with an atmospheric pressure chemical ionization (APCI) probe for sample ionization. The APCI probe was operated in positive mode and had a source voltage of 6 kV, source current of 5  $\mu$ A, vaporizer temperature of 450 °C, nitrogen sheath gas flow of 80 (arb.), no auxiliary gas, capillary temperature of 150 °C, capillary voltage of 3 V and source-induced dissociation of 10%. Peaks were separated on an analytical scale Luna C18 (2) column using a mobile phase of 10 mM ammonium acetate–acetonitrile (30:70, v:v) at a flow rate of 1 mL/min. Samples (approximately 10  $\mu$ g/mL) were prepared in water–acetonitrile (30:70, v:v). The injection volume was 100  $\mu$ L, column temperature was 40 °C, and detection wavelengths were 245 and 280 nm. Data were acquired through Thermo's Xcalibur software (Version 1.2).

NMR spectra were obtained on Varian Unity Inova 300 or 600 MHz spectrometers (Palo Alto, CA) at 25 °C. At the 600 MHz spectrometer, <sup>1</sup>H-1D, diffusion, 1D TOCSY, and 2D DQF-COSY, TOCSY, T-ROESY, and <sup>1</sup>H-<sup>13</sup>C correlation spectra of HSQC and HMBC were acquired on H<sub>2</sub>B<sub>1a</sub>, B<sub>2a</sub>, 24-demethyl H<sub>2</sub>B<sub>1a</sub>, and 24a-hydroxy-B<sub>2a</sub> isomer in CDCl<sub>3</sub>. <sup>1</sup>H-1D spectra were obtained for both 3'-demethyl and 3''-demethyl H<sub>2</sub>B<sub>1a</sub> on the 300 MHz spectrometer in CDCl<sub>3</sub>.

### 2.3. Preparation of samples

Samples for analytical scale separations were prepared by diluting 30 mg of bulk drug in 100 mL of methanol. Samples for preparative-scale separations were prepared by diluting 500 mg in 10 mL of methanol.

## 3. Results and discussion

The USP Monograph for ivermectin utilizes an Apex ODS HPLC column for assay and related substances [29]. Injecting a standard onto this column according to the conditions outlined in the USP reveals two main peaks attributed to H<sub>2</sub>B<sub>1b</sub> (~10.5 min) and H<sub>2</sub>B<sub>1a</sub> (~12.8 min, peak max 610 mV) along with numerous low-level peaks (Fig. 2). Several of these low level peaks have been molecularly characterized. They have consistently been found to be either process impurities origi-

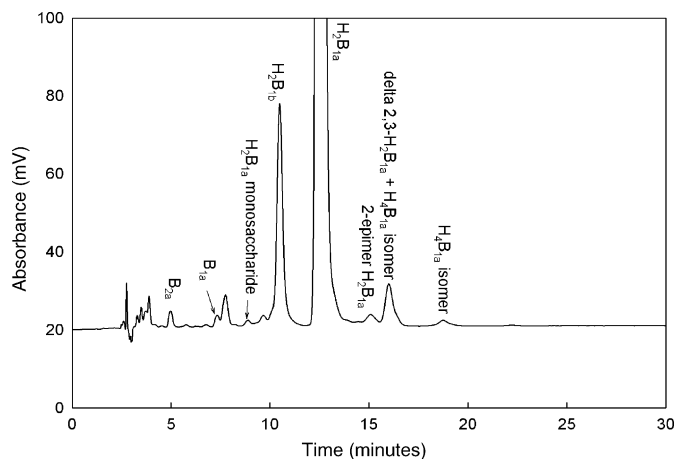


Fig. 2. Chromatogram of bulk ivermectin: Apex ODS (250 mm  $\times$  4.6 mm ID, 5  $\mu$ m), water:methanol:acetonitrile (12:35:53, v:v:v), 1.0 mL/min, 40 °C column temperature, 20- $\mu$ L injection volume, 245-nm detection wavelength.

inating from the avermectin starting material (B<sub>1a</sub> and B<sub>2a</sub>) that was used in the synthesis of ivermectin, or degradation products of ivermectin (2-epimer H<sub>2</sub>B<sub>1a</sub> and  $\Delta^{2,3}$ -H<sub>2</sub>B<sub>1a</sub>). Pharmaceutical grade avermectin is purified from *Streptomyces Avermetilis* fermentations via extraction, precipitation, and large-scale chromatography. Although the process yields avermectin of high purity some known and unknown impurities are still present and are not removed during purification after catalytic hydrogenation of avermectin to ivermectin. Chromatography on a Luna column was explored in order to allow for preparative-scale separations on already available columns in our laboratory. Separation of the various peaks present in ivermectin was achieved on a Phenomenex Luna C18 column (150 mm  $\times$  4.6 mm ID, 3  $\mu$ m) with a mobile phase consisting of water:acetonitrile (30:70, v/v) at a flow rate of 1.0 mL/min. The peaks from the Apex ODS column were correlated with the peaks from the Luna C18 column by comparing LC/UV data (Fig. 3). Peak retention times were compared to those of known ivermectin degradation products to separate them from impurities. The UV absorption profiles of impurity peaks were compared to the UV spectrum of ivermectin and they were identical with the UV spectra obtained with ivermectin H<sub>2</sub>B<sub>1a</sub> and H<sub>2</sub>B<sub>1b</sub>. The unknown impurities with area responses >0.2% relative to the combined area response of H<sub>2</sub>B<sub>1a</sub> and H<sub>2</sub>B<sub>1b</sub> were labeled unknowns 1, 2, 3, and 4 in the order of their appearance.

Fractions from preparative ivermectin separations containing these unknowns were concentrated using a rotary evaporator and then reinjected on the analytical scale Luna C18 column to confirm their identity. Once the identity was confirmed, the fractions were evaporated using a rotary evaporator and further dried in high vacuum.

Mass-spectrometric data were obtained from all peaks eluting from the analytical size Luna column using a Thermo-Finnegan LCQ operating under conditions listed in the experimental section. The fragmentation of ivermectin is similar to the fragmentation of avermectins, both of which have been described extensively in the literature [30–32]. The three main fragmentation species for ivermectin (and avermectin) are the loss of

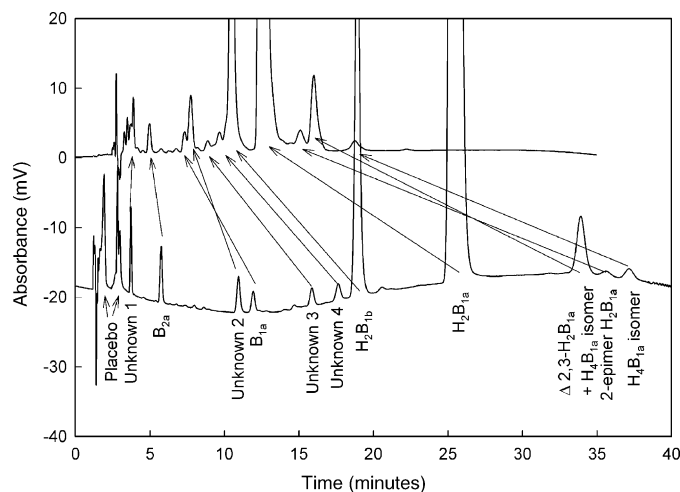


Fig. 3. Chromatograms of bulk ivermectin: top chromatogram: Apex ODS (250 mm  $\times$  4.6 mm ID, 5  $\mu$ m), water:methanol:acetonitrile (12:35:53, v:v:v), 1.0 mL/min, 40  $^{\circ}$ C column temperature, 20  $\mu$ L injection volume, 254 nm detection wavelength. Bottom chromatogram: Phenomenex Luna C18 (2) (150 mm  $\times$  4.6 mm ID, 3  $\mu$ m), water–acetonitrile (30:70, v:v), 1.0 mL/min, 40  $^{\circ}$ C column temperature, 100- $\mu$ L injection volume, 245-nm detection wavelength.

a monosaccharide unit, the loss of a disaccharide unit, and a McLafferty rearrangement with a subsequent fragmentation of the aglycon unit (Scheme 1). Under LC/MS conditions used in this paper  $H_2B_{1a}$  forms a precursor ion adduct ( $M + NH_4^+$ ,  $m/z$  892.3). The loss of a monosaccharide unit or disaccharide unit corresponds to product ions  $m/z$  713.4 and 568.9, respectively. Loss of the disaccharide moiety produces the aglycon, which

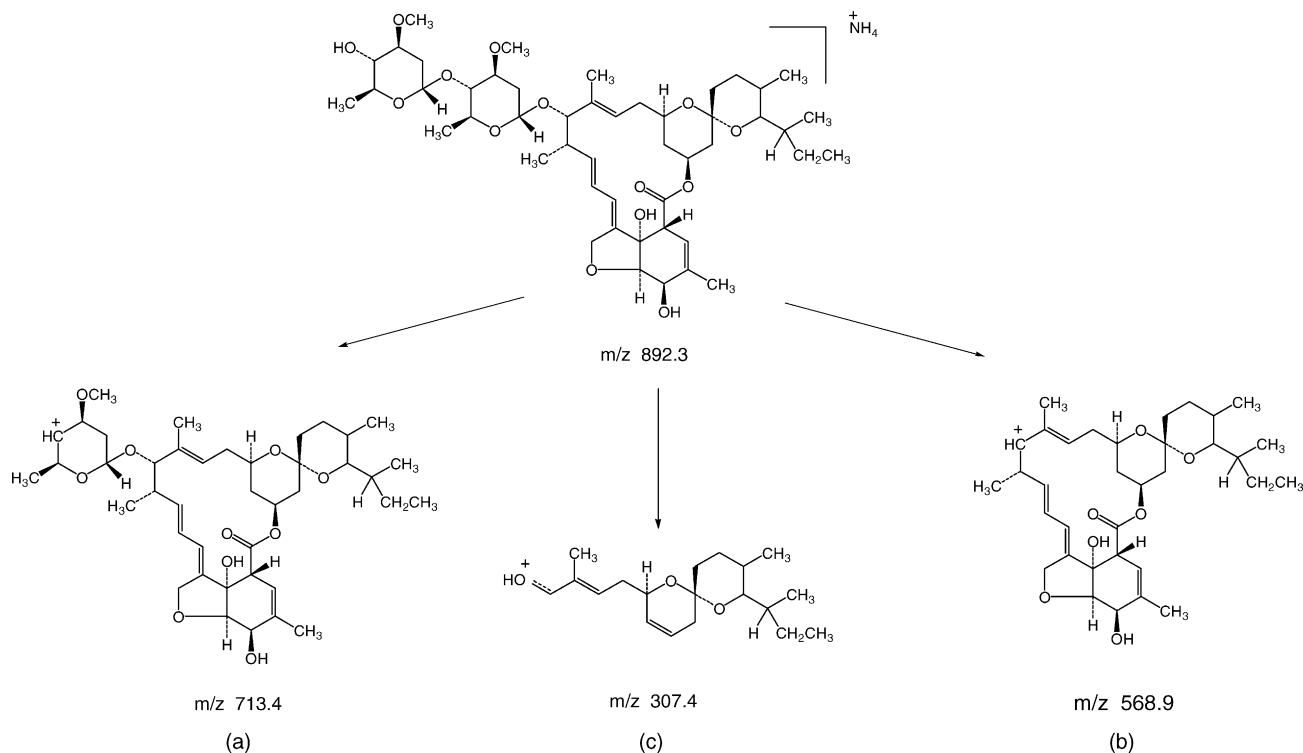
undergoes a McLafferty type rearrangement to produce a  $m/z$  307.4 fragment. Under the same experimental conditions, avermectin  $B_{1a}$  and the respective product ions mentioned above produce MS signals with masses of 2 Da less.

Proton chemical shifts were acquired by NMR of  $H_2B_{1a}$  and  $B_{2a}$  were acquired as references to aid in the elucidation of two of the unknowns and are summarized in Table 1. The spectra of  $H_2B_{1a}$ ,  $B_{2a}$ , unknown 1, and unknown 4 are also provided as reference (Figs. 4 and 5).  $B_{2a}$  was acquired as a reference because one of the unknowns was shown to be an isomer of  $B_{2a}$ . This isomer will be discussed in the following subsection.

### 3.1. Unknown 1—24a-hydroxy $B_{2a}$ isomer

LC/MS on unknown 1 reveals a ( $M + NH_4^+$ ) precursor ion with an  $m/z$  of 907.8. Product ions in the spectrum of unknown 1 have  $m/z$  728.6, 585.0, and 323.1 (Table 2). Both the precursor and product ions are 16 Da larger than those ions observed for  $H_2B_{1a}$  indicating an additional oxygen atom in the molecule. The increase of 16 Da in the smallest product ion discussed indicates that the oxygen resides in fragment “c” shown in Scheme 1. Additionally, examination of further LC/MS data revealed that the fragmentation of unknown 1 was identical to  $B_{2a}$  indicating a possible isomer. NMR on unknown 1 revealed it to be an isomer of  $B_{2a}$  with the OH residing at the 24a position.

The most striking observation in the 1D NMR spectrum (Figs. 4C and 5C) of the 24a-hydroxy  $B_{2a}$  isomer in  $CDCl_3$  was the appearance of the 24a methylene protons at 3.615



Scheme 1. Three major fragmentation species for  $H_2B_{1a}$ .

Table 1  
Proton chemical shift assignments ( $\delta_{\text{H}}$  ppm) of  $\text{H}_2\text{B}_{1\text{a}}$ , 24a-hydroxy  $\text{B}_{2\text{a}}$  isomer, 24-demethyl  $\text{H}_2\text{B}_{1\text{a}}$  and  $\text{B}_{2\text{a}}$  in  $\text{CDCl}_3$

Assignment		$\text{H}_2\text{B}_{1\text{a}}$	$\text{B}_{2\text{a}}$	Unknown 1 (24a-hydroxy $\text{B}_{2\text{a}}$ isomer)	Unknown 2 (24-demethyl $\text{B}_{2\text{a}}$ )
2	CH	3.288 ( $J=2.2$ )	3.294	3.294	3.286
3	CH	5.428	5.425	5.430	5.417
4a	CH <sub>3</sub>	1.878	1.881	1.880	1.878
5	CH	4.296 ( $J=3.9$ )	4.296 ( $J=7.2$ )	4.297	4.296
5a	–OH	2.349	2.336	2.351	2.337
6	CH	3.973 ( $J=6.3$ )	3.971	3.973	3.972
7a	–OH	4.127	3.977	4.095	4.141
8a	CH <sub>2</sub>	4.696 ( $J=14.3, 2.2$ ), 4.669 ( $J=14.4, 2.0$ )	4.694, 4.672	4.697, 4.671	4.697, 4.667
9	CH	5.859 ( $J=10.3$ )	5.859	5.865	5.858
10	CH	5.731	5.741	5.736	5.734
11	CH	5.737	5.747	5.739	5.738
12	CH	2.521	2.527	2.523	2.523
12a	CH <sub>3</sub>	1.167 ( $J=7.0$ )	1.170	1.166	1.168
13	CH	3.945	3.961	3.945	3.947
14a	CH <sub>3</sub>	1.501	1.505	1.501	1.504
15	CH	4.988 ( $J=10.9$ )	4.978 ( $J=7.0$ )	4.981	5.001
16	CH <sub>2</sub>	2.328, 2.281 ( $J=11.4$ )	2.336, 2.307	2.326, 2.279	2.328, 2.279
17	CH	3.676 ( $J=10.8, 3.1$ )	3.775	3.677	3.673
18	CH <sub>2</sub>	1.765 ( $J=8.0$ ), 0.823 ( $J=12.1$ )	1.782, 0.870	1.777, 0.836	1.777, 0.826
19	CH	5.362 ( $J=16.3, 11.4, 5.1$ )	5.332	5.358	5.416
20	CH <sub>2</sub>	1.978 ( $J=8.2, 3.9$ ), 1.358 ( $J=11.8$ )	2.005, 1.428	1.998, 1.377	1.985, 1.369
22	CH <sub>2</sub>	1.658 ( $J=12.8$ ), 1.478	1.986, 1.672 ( $J=10.8, 3.3$ )	1.747, 1.501	1.638, 1.407
23		CH <sub>2</sub> 1.516, 1.516	CH 3.776	CH <sub>2</sub> 1.711	CH <sub>2</sub> 1.841, 1.598
23			C–OH 3.502		
24		CH 1.516	CH 1.624	CH 1.652	CH <sub>2</sub> 1.545, 1.263
24a		CH <sub>3</sub> 0.790 ( $J=5.7$ )	CH <sub>3</sub> 0.910	CH <sub>2</sub> 3.615, 3.470	
24a				–OH 4.623	
25	CH	3.221	3.573 ( $J=10.6$ )	3.485	3.412
26	CH	1.553	1.555	1.578	1.378
26a	CH <sub>3</sub>	0.858 ( $J=6.8$ )	0.880	0.907	0.943
27	CH <sub>2</sub>	1.443, 1.417	1.496	1.476, 1.433	1.538, 1.173
28	CH <sub>3</sub>	0.935 ( $J=7.4$ )	0.967	0.941	0.908
1'	CH	4.778 ( $J=3.4$ )	4.765	4.773	4.798
2'	CH <sub>2</sub>	2.229 ( $J=8.3, 4.6$ ), 1.560	2.217, 1.585	2.214, 1.571	2.249, 1.589
3'	CH, –OCH <sub>3</sub>	3.624, 3.434	3.618, 3.433	3.624, 3.430	3.624, 3.424
4'	CH	3.243	3.246	3.246 ( $J=9.0$ )	3.247
5'	CH	3.833	3.829	3.831	3.830
6'	CH <sub>3</sub>	1.259 ( $J=6.2$ )	1.259	1.259	1.260
1''	CH	5.397 ( $J=3.5$ )	5.395	5.395	5.398
2''	CH <sub>2</sub>	2.337, 1.518	2.332, 1.536	2.337, 1.528	2.338, 1.530
3''	CH, –OCH <sub>3</sub>	3.482, 3.424	3.492, 3.423	3.485, 3.423	3.485, 3.441
4''	CH, –OH	3.168 ( $J=9.1$ ), 2.481	3.169, 2.463	3.170, 2.478	3.170, 2.467
5''	CH	3.772	2.463	3.771	3.773
6''	CH <sub>3</sub>	1.280 ( $J=6.2$ )	1.280	1.280	1.281

$\delta_{\text{H}}$  referenced to TMS at 0.00 ppm.

Table 2  
Characteristic fragments for the four major impurities found in ivermectin

	$\text{H}_2\text{B}_{1\text{a}}$	$\text{B}_{2\text{a}}$	24a-Hydroxy $\text{B}_{2\text{a}}$ isomer	3'-Demethyl $\text{H}_2\text{B}_{1\text{a}}$ (3'-demethyl $\text{B}_{1\text{a}}$ )	3''-Demethyl $\text{H}_2\text{B}_{1\text{a}}$ (3''-demethyl $\text{B}_{1\text{a}}$ )	24-Demethyl $\text{H}_2\text{B}_{1\text{a}}$ (24-demethyl $\text{B}_{1\text{a}}$ )
$\text{M} + \text{NH}_4^+$	892.3	907.7	907.8	877.8 (875.9)	877.7 (875.7)	877.7 (875.8)
a	713.4	728.6	728.7	699.1 (697.2)	712.5 (710.6)	698.5 (696.6)
b	568.9	584.9	584.8	569.1 (567.1)	568.7 (566.6)	554.6 (552.6)
c	307.4	323.1	323.2	307.4 (305.4)	307.1 (305.1)	293.0 (291.1)

$\text{H}_2\text{B}_{1\text{a}}$  and  $\text{B}_{2\text{a}}$  are also shown for ease of comparison. Numbers in parenthesis are  $m/z$  values for impurities in ivermectin.

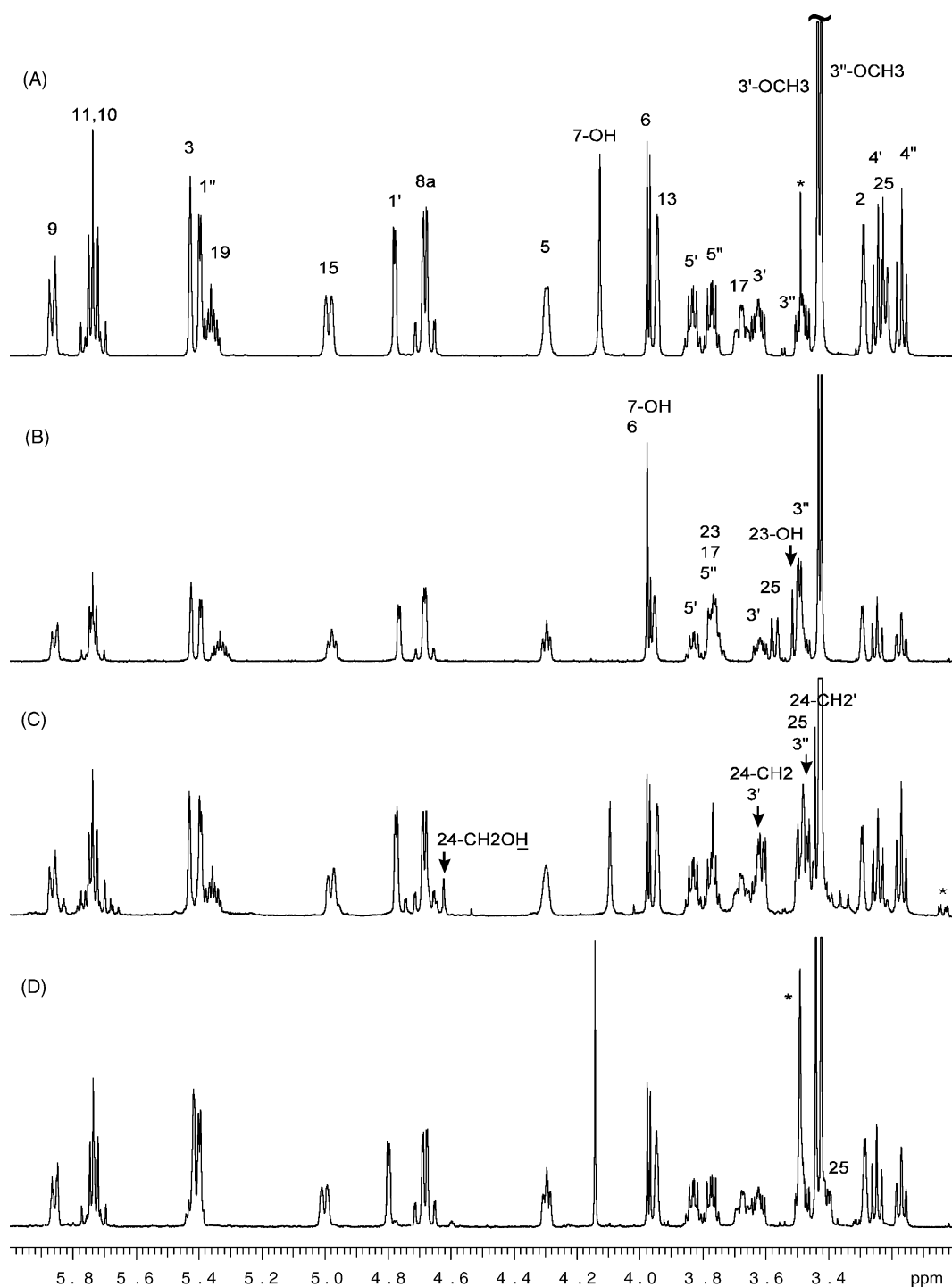


Fig. 4.  $^1\text{H}$  NMR Spectra in the region of 3.0–6.0 ppm for  $\text{H}_2\text{B}_{1a}$  (A),  $\text{B}_{2a}$  (B), 24a-hydroxy  $\text{B}_{2a}$  isomer (C), and 24-demethyl  $\text{H}_2\text{B}_{1a}$  (D). Impurity and solvent peaks are indicated by asterisks.

and 3.470 ppm, and the replacement of one methyl peak around 0.8 ppm with two small doublet peaks. In the HMBC spectrum (not shown), the above-mentioned methylene protons had three-bond correlation to C-23 and C-25, and two-bond correlation to C-24. The H–C correlation peak of H-23 in HSQC (not shown) integrated to more than one proton. A reasonable

structure that fits to the above data suggests hydroxylation at the 24a methyl group, which could explain why the methyl peak present in  $\text{H}_2\text{B}_{1a}$  and  $\text{B}_{2a}$  1D spectra did not appear in the 1D spectrum. Finally, the two proton doublet peaks around 0.84 ppm had the same correlation features in the HMBC as those of 24a and 26a in  $\text{H}_2\text{B}_{1a}$ .

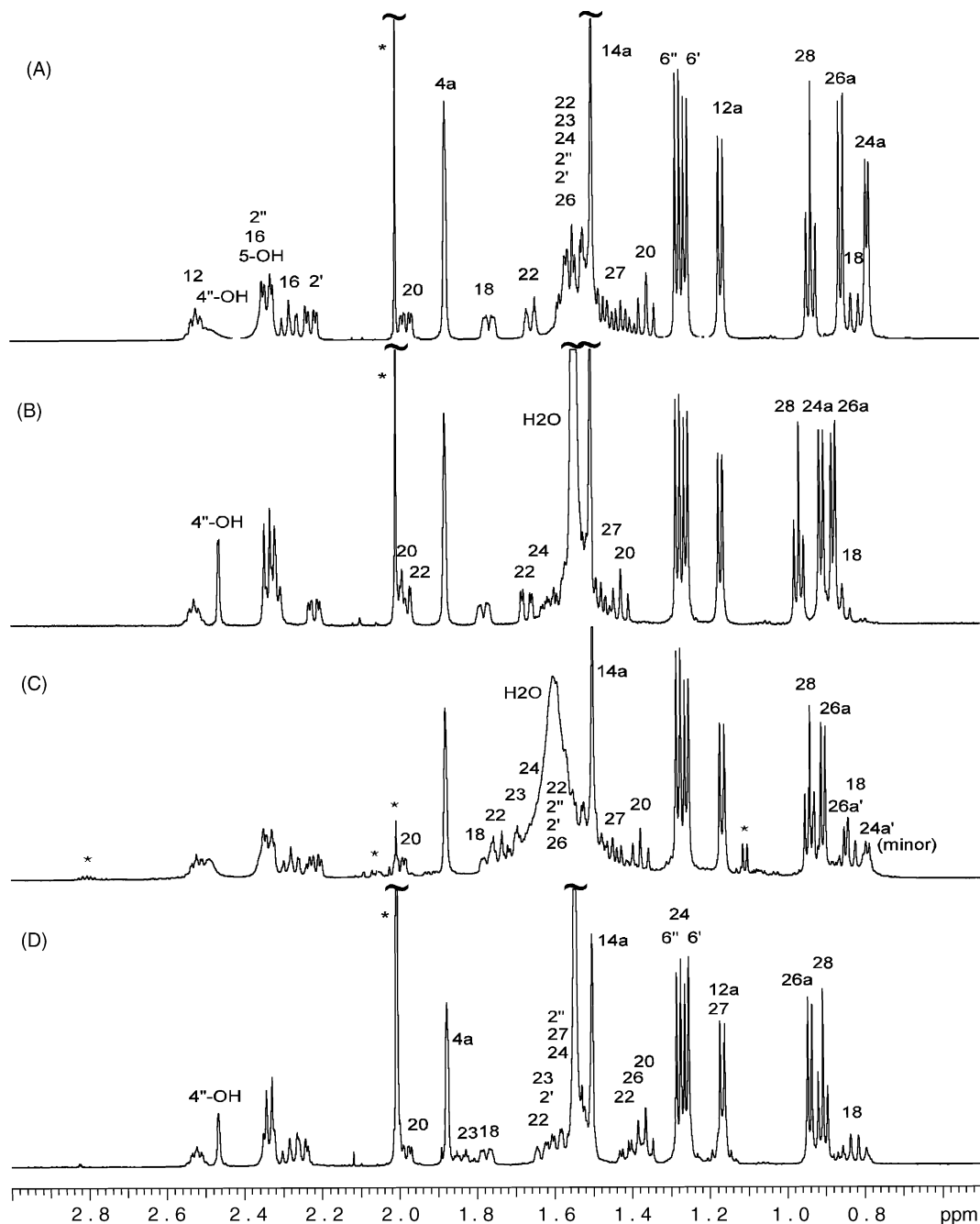


Fig. 5. <sup>1</sup>H NMR Spectra in the region of 0–3.0 ppm for H<sub>2</sub>B<sub>1a</sub> (A), B<sub>2a</sub> (B), 24a-hydroxy B<sub>2a</sub> isomer (C), and 24-demethyl H<sub>2</sub>B<sub>1a</sub> (D). Impurity and solvent peaks are indicated by asterisks.

### 3.2. Unknown 2—3'-demethyl-H<sub>2</sub>B<sub>1a</sub>

LC/MS of unknown 2 showed precursor and product ions  $m/z$  877.8 ( $M + NH_4^+$ ), 699.1, 569.1, and 307.1 (Table 2). The precursor ion of unknown 2 is 14 Da less, possibly a demethyl product, than H<sub>2</sub>B<sub>1a</sub> with the “a” fragment (Scheme 1) also being 14 Da less. The “b” and “c” fragments both have the same  $m/z$  as the corresponding fragments of H<sub>2</sub>B<sub>1a</sub>. The “a” fragment being 14 Da less than the corresponding monosaccharide of H<sub>2</sub>B<sub>1a</sub> indicates the loss of 14 is occurring in the second sugar ring. NMR data reveal that the loss of a methyl group is occurring at

the C-3' position as evidenced by the loss of the NMR singlet at 3.434 ppm.

### 3.3. Unknown 3—3''-demethyl-H<sub>2</sub>B<sub>1a</sub>

Unknown 3 has a precursor ion  $m/z$  877.7 Da ( $M + NH_4^+$ ), 14 Da less than H<sub>2</sub>B<sub>1a</sub> (Table 2) and which like unknown 2 corresponds to a demethylated impurity. The three largest fragments, “a”, “b”, and “c” all have the same  $m/z$  as the H<sub>2</sub>B<sub>1a</sub> fragments indicating that the loss of the methyl group occurs on the first sugar ring. NMR data reveal that the loss

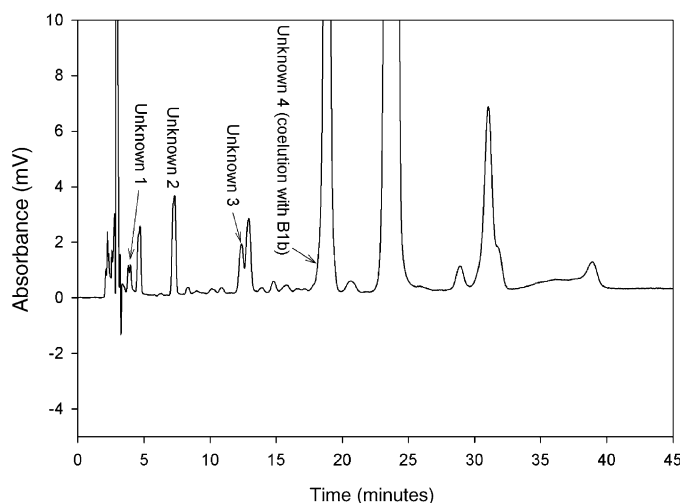


Fig. 6. Chromatogram of bulk avermectin: waters symmetry C18 (150 mm  $\times$  4.6 mm ID, 5  $\mu$ m); mobile phase A: water–acetonitrile (50:50, v:v); mobile phase B: acetonitrile, 1.5 mL/min, 35  $^{\circ}$ C column temperature, 20- $\mu$ L injection volume, 245-nm detection wavelength. Gradient time: 0, 10, 25, 27.5, 32.5, 35, 45; % B: 10, 20, 20, 50, 50, 10, 10.

of a methyl group is occurring at the C-3'' position as evidenced by the loss of the NMR singlet at 3.424 ppm. Both C-3' and C-3'' demethylated products have been observed during elucidation studies on the biosynthesis of avermectins [35].

#### 3.4. Unknown 4—24-demethyl- $H_2B_{1a}$

The precursor ion for unknown 4 is  $m/z$  877.7 ( $M + NH_4^+$ ) (Table 2). Like unknowns 2 and 3 the loss of 14 Da indicates a probable demethylated product. The “a”, “b”, and “c” fragments of unknown 4 are all 14 Da less than their corresponding fragments for  $H_2B_{1a}$ . These data indicate that the “c” fragment is demethylated at the C-14, -26a, or -24a position. The first attempt by MS could not determine which methyl group, C-14, -24a, or -26a, existed in the structure. NMR studies (Fig. 4D) on a relatively pure fraction of unknown 4 subsequently revealed the 24a position is demethylated. In NMR, by selectively exciting the methyl peak at 0.908 ppm, followed by different periods of TOCSY mixing, magnetization traveled from 28a methyl to H-27, then to H-26, and finally to H-26a methyl protons. These data indicate that the 24a methyl group was not in the structure. The HSQC spectrum showed methylene H–C correlations for H-22, H-23 and H-24.

We hypothesized that the impurities arose prior to the catalytic hydrogenation of avermectin  $B_{1a}$  and  $B_{1b}$ . Examining the impurity profile of bulk avermectin  $B_{1a}$  and  $B_{1b}$  reveal that these four impurities do indeed arise prior to the catalytic hydrogenation and speculatively during the biosynthesis of avermectin. All four impurities are present in bulk avermectin and they can be separated from known process impurities using HPLC as shown in Fig. 6. As mentioned in the introduction, the fermentation of *Streptomyces avermitilis* produces a variety of different avermectins. The avermectins are separated from the

fermentation broth through a series of solvent extractions and precipitations. Four major avermectins – A1, B1, A2 and B2 – are obtained in similar yields in the process. Separation of these four compound groups from each other can be further achieved, however they are always mixtures of the respective major “a” and minor “b” components. Pharmaceutical grade avermectin B1 is obtained by subsequent large-scale chromatography. Although these series of steps provide relatively pure B1, there are numerous low-level process impurities in the final product.

The avermectin bulk impurities can be readily attributed to the biosynthesis of the avermectins. Subsequently, the ivermectin process impurities are the result of catalytic hydrogenation of the avermectin impurities during the ivermectin synthesis. The biosynthesis of avermectin has been completely elucidated [35,36] and can be divided into three major steps: (1) formation of the initial polyketide aglycon, (2) modification of the initial polyketide aglycon to form the avermectin aglycon, and (3) glycolysation of the aglycon to form the avermectins. The initial polyketide is formed by a series of 12 acyl condensations in the order of P-A-A-A-A-P-P-A-P-A-P-A (acetyl- or propionyl-CoA) to 2-methylbutyrate or isobutyrate (a or b components) which are orchestrated by a series of polyketide synthetases. Non-specific head-to-tail condensation of acetyl-CoA to the sulfur linked methylbutyryl-acyl carrying protein of the first polyketide synthetase unit produces the precursor from which the 24-demethyl  $A_{1a}$  arises (Fig. 7). Similarly, condensation of 3-hydroxypropionyl-CoA to the 2-methylbutyryl starter unit produces 24-hydroxyl  $A_{1a}$ . The formation of this impurity may also be the result of a hydroxylation of the aglycon or  $A_{1a}$  by a monooxygenase. Hydroxylation of the 24-methyl group of A1 to form the 24-hydroxyl compound was reported in hepatic cells [3].

The last step in the avermectin biosynthesis involves glycosylation of the 13-OH group of the aglycons with TDP-oleandrose to form the avermectin monosaccharides. These are then glycosylated by a specific glycosidase with another molecule of TDP-oleandrose at the 4'-OH group to form the avermectins. L-Oleandrose is enzymatically derived from D-glucose. One of the key intermediates is L-oleandrose-1-phosphate, which is methylated at the C3 position by a substrate specific methyltransferase that utilizes S-adenosyl-L-methionine. In the biosynthetic pathway leading to the regular avermectins, this C3 methylated sugar is then enzymatically condensed with TTP to form TDP-oleandrose and pyrophosphate. Condensation of the 3'-methyl-TDP-oleandrose with avermectin aglycons produce the expected 3'-methyl monosaccharides which are then glycosylated with TDP-oleandrose to form the normal avermectins (Fig. 8). In the case that aglycon glycolysation is performed with 3'-demethyl-TDP-oleandrose, the respective 3'-demethyl-monosaccharides are formed. Further glycosylation of these yields the 3'-demethyl-avermectins. Similarly, glycosylation of the (3'-methyl) avermectin monosaccharides with 3'-demethyl-TDP yields 3''-demethyl-avermectins. The likelihood of incorporation of two 3'-demethylated oleandrose moieties can be considered small since the enzyme that performs this step may exhibit a high substrate specificity for the 3'-methylated-TDP-



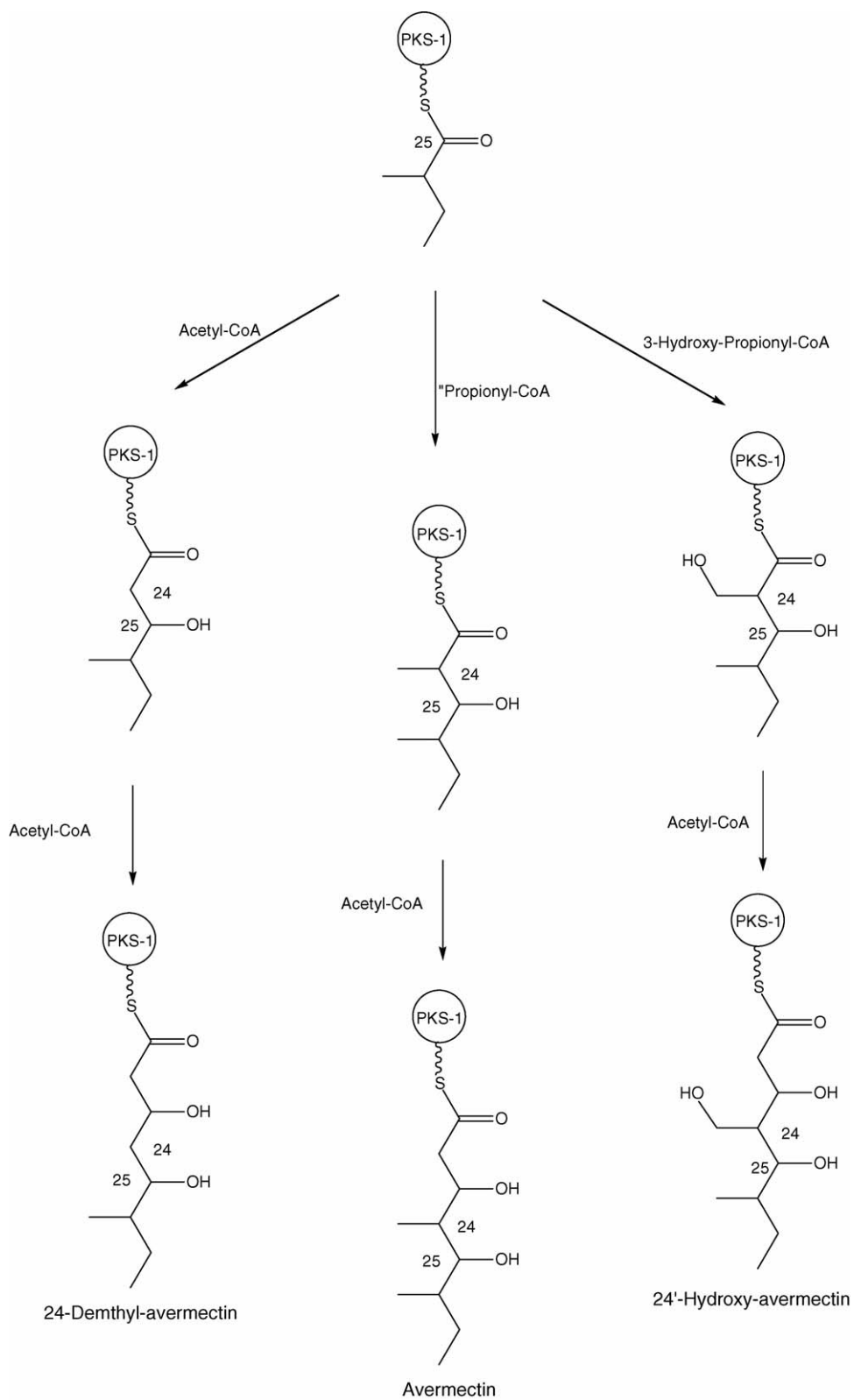


Fig. 7. Biosynthetic origin of 24-demethyl avermectin and 24'-hydroxy avermectin.

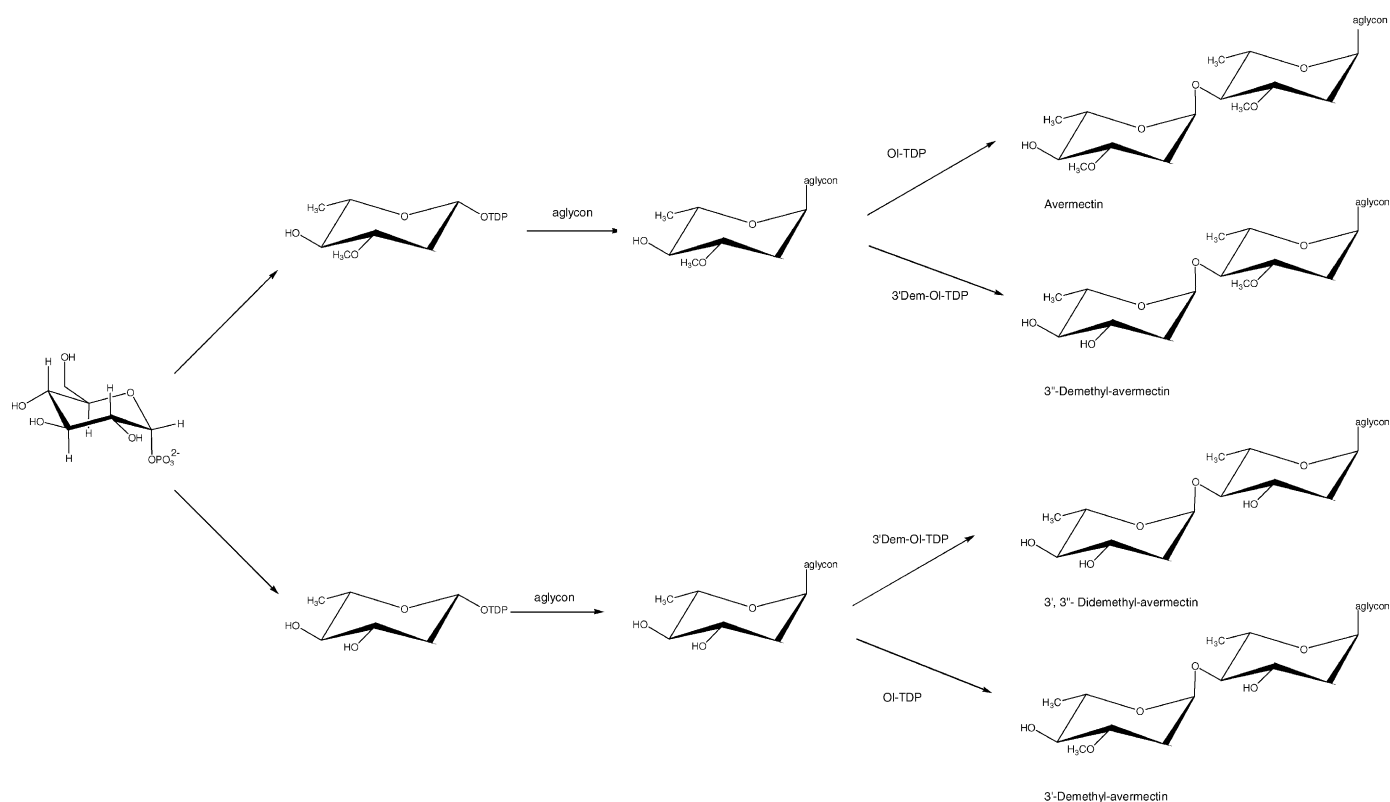


Fig. 8. Biosynthetic origin of 3'- and 3''-demethyl avermectin.

oleandrose. Interestingly, demethylated ivermectin H<sub>2</sub>A<sub>1a</sub> compounds were found in drug metabolism studies of ivermectin [37,38].

#### 4. Conclusion

Four process impurities in bulk ivermectin, 24a-hydroxy B<sub>2a</sub> isomer, 3'-demethyl H<sub>2</sub>B<sub>1a</sub>, 3''-demethyl H<sub>2</sub>B<sub>1a</sub> and 24-demethyl H<sub>2</sub>B<sub>1a</sub> have been identified and characterized by LC/MS and NMR. The precursors to 3'-demethyl H<sub>2</sub>B<sub>1a</sub>, 3''-demethyl H<sub>2</sub>B<sub>1a</sub> and 24-demethyl H<sub>2</sub>B<sub>1a</sub> along with 24a-hydroxy B<sub>2a</sub> isomer are present in bulk avermectin indicating that these impurities are a product of the biosynthesis of avermectin.

#### References

- [1] R.W. Burg, B.M. Miller, E.E. Baker, J. Birnbaum, S.A. Currie, R. Hartman, Y.L. Kong, R.L. Monaghan, G. Olson, I. Putter, J.B. Tunac, H. Wallick, E.O. Stapely, R. Oiwa, S. Ōmura, *Antimicrob. Agents Chemother.* 15 (1979) 361–367.
- [2] C. Bagner, A.S. Wildman, European Patent 0082674 A2 (1982).
- [3] H.G. Davies, R.H. Green, *Nat. Prod. Rep.* 3 (1986) 87–121.
- [4] T.W. Miller, L. Chalet, D.J. Cole, L.J. Cole, J.E. Flor, R.t. Goegelman, V.P. Gullo, H. Joshua, A.J. Kempf, W.R. Krellwitz, R.L. Monaghan, R.E. Ormond, K.E. Wilson, G. Alberts-Schoenberg, I. Putter, *Antimicrob. Agents Chemother.* 15 (1979) 368–371.
- [5] J.C. Chabala, M.H. Fisher, United States Patent 4,199,659 (1980).
- [6] M. Strobel, United States Patent 20050009762 A1 (2005).
- [7] G.R. Huber, D.R. Jones, J.C. Kuenzi, K.D. Kuenzi, United States Patent 6,716,448 B2 (2004).
- [8] C. Harvey, United States Patent 6,663,879 B2 (2003).
- [9] J. Bouvier, C. Kolly, European Patent 1244359 B1 (2000).
- [10] J. Kinzell, M.T. Baker, D. Hepler, European Patent 1,154,755 A1 (2000).
- [11] B.W. Hak, European Patent 0,617,892 A1 (1993).
- [12] M.A. Aziz, S. Diallo, I.M. Diop, M. Lariviere, M. Porta, *Lancet* 2 (1982) 171–173.
- [13] M.A. Aziz, S. Diallo, M. Lariviere, I.M. Diop, M. Porta, P. Gaxotte, *Lancet* 2 (1982) 1456–1457.
- [14] D. Nalin, M. Aziz, D. Neu, G. Ruiz-Palacios, C. Naquira, *Annu. Meet. Am. Soc. Microbiol.: Abstr. A-101* (1987) 17.
- [15] V. Manetta, G.R. Watkins, World Patent 2004093886 A1 (2004).
- [16] L.D. Parks, European Patent 1294375 A2 (2001).
- [17] M.D. Soll, K. Kumar, R.P. Waranis, N. Shub, United States Patent 2004198676 (2004).
- [18] J. Høglund, C. Ganheim, S. Alenius, *Vet. Parasitol.* 114 (2003) 205–214.
- [19] L.B. Lowe, J.T. Rothwell, World Patent 2003024223 (2003).
- [20] G. Cringoli, L. Rinaldi, V. Veneziano, G. Capelli, *Vet. Parasitol.* 112 (2003) 203–209.
- [21] A. Nodtvedt, I. Dohoo, J. Sanchez, G. Conboy, L. DesCoteaux, G. Keefe, *Vet. Parasitol.* 105 (2002) 191–206.
- [22] A.S. Huq, Z.J. Shao, K.J. Varma, United States Patent 6,486,128 (2002).
- [23] D.A. Potter, L. Foss, R.E. Baumler, D.W. Held, *Pest Manage. Sci.* 61 (2005) 3–15.
- [24] G.P. Gupta, S. Rani, A. Birah, M. Raghuraman, *Pest Res. J.* 16 (2004) 45–47.
- [25] K. Takai, T. Suzuki, K. Kawazu, *Pest Manage. Sci.* 59 (2003) 365–370.
- [26] I. Ishaaya, S. Konsedalov, A.R. Horowitz, *Pest Manage. Sci.* 58 (2002) 1091–1095.
- [27] C.J. Dutton, S.P. Gibson, A.C. Goudie, K.S. Holdom, M.S. Pacey, J.C. Ruddock, J.D. Bu'Lock, M.K. Richards, *J. Antibiot.* 44 (1991) 357–365.
- [28] *Ph. Eur.*, 5th ed., 2005, pp. 1854–1856.
- [29] USP XXXV, US Pharmacopeial Convention, Rockville, MD, 2005, pp. 1093–1094.
- [30] L. Howells, M.J. Sauer, *Analyst* 126 (2000) 155–160.

- [31] G. Albers-Schönberg, B.H. Arison, J.C. Chabala, A.W. Douglas, P. Eskola, M.H. Fisher, A. Lusi, H. Mrozik, J.L. Smith, R.L. Tolman, *J. Am. Chem. Soc.* 103 (1981) 4216–4221.
- [32] D.W. Fink, in: K. Florey, A.A. Al-Badr, G.S. Brenner, G.A. Brewer (Eds.), *Analytical Profiles of Drug Substances*, Academic Press, San Diego, 1988, pp. 155–184.
- [33] L. Gianelli, G.C. Mellerio, E. Siviero, A. Rossi, W. Cabri, L. Sogli, *Rapid Commun. Mass Spectrom.* 14 (2000) 1260–1265.
- [34] A.J. Faulkner, Q. Wang, P. DeMontigny, J.S. Murphy, *J. Pharm. Biomed. Anal.* 15 (1997) 523–526.
- [35] H. Ikeda, S. Ōmura, *Chem. Rev.* 97 (1997) 2591–2609.
- [36] D.E. Cane, T. Liang, L. Kaplan, M.K. Nallin, M.D. Schulman, O.D. Hensens, A.W. Douglas, G. Albers-Schönberg, *J. Am. Chem. Soc.* 105 (1983) 4110–4112.
- [37] S.H.L. Chiu, E. Sestokas, R. Taub, J.L. Smith, B. Arison, A.Y.H. Lu, *Drug. Metab. Dispos.* 12 (1984) 464–469.
- [38] G.T. Miwa, J.S. Walsh, W.J.A. VandenHeuvel, B. Arison, E. Sestokas, R. Buhs, A. Rosegay, S. Avermitilis, A.Y.H. Lu, M.A.R. Walsh, R.W. Walker, R. Taub, T.A. Jacob, *Drug. Metab. Dispos.* 10 (1982) 268–274.